TISSUE ENGINEERING: Part A
Volume 22, Numbers 9 and 10, 2016

DOI: 10.1089/ten.tea.2015.0379

termis
Tissue Engineering
& Regenerative Medicine
International Society

ORIGINAL ARTICLE

In Vivo Functional Evaluation of Tissue-Engineered Vascular Grafts Fabricated Using Human Adipose-Derived Stem Cells from High Cardiovascular Risk Populations

Jeffrey T. Krawiec, PhD,[1,2,*] Justin S. Weinbaum, PhD,[1,2,*] Han-Tsung Liao, MD, PhD,[3,4] Aneesh K. Ramaswamy, MS,[1,2] Dominic J. Pezzone, BS,[1] Alexander D. Josowitz, BS,[1] Antonio D'Amore, PhD,[1,2,5,6] J. Peter Rubin, MD,[2,3] William R. Wagner, PhD,[1,2,5,7] and David A. Vorp, PhD[1,2,5,7,8]

Many preclinical evaluations of autologous small-diameter tissue-engineered vascular grafts (TEVGs) utilize cells from healthy humans or animals. However, these models hold minimal relevance for clinical translation, as the main targeted demographic is patients at high cardiovascular risk such as individuals with diabetes mellitus or the elderly. Stem cells such as adipose-derived mesenchymal stem cells (AD-MSCs) represent a clinically ideal cell type for TEVGs, as these can be easily and plentifully harvested and offer regenerative potential. To understand whether AD-MSCs sourced from diabetic and elderly donors are as effective as those from young nondiabetics (i.e., healthy) in the context of TEVG therapy, we implanted TEVGs constructed with human AD-MSCs from each donor type as an aortic interposition graft in a rat model. The key failure mechanism observed was thrombosis, and this was most prevalent in grafts using cells from diabetic patients. The remainder of the TEVGs was able to generate robust vascular-like tissue consisting of smooth muscle cells, endothelial cells, collagen, and elastin. We further investigated a potential mechanism for the thrombotic failure of AD-MSCs from diabetic donors; we found that these cells have a diminished potential to promote fibrinolysis compared to those from healthy donors. Together, this study served as proof of concept for the development of a TEVG based on human AD-MSCs, illustrated the importance of testing cells from realistic patient populations, and highlighted one possible mechanistic explanation as to the observed thrombotic failure of our diabetic AD-MSC-based TEVGs.

Introduction

Cardiovascular disease is the leading cause of death within the United States. Approximately 600,000 surgical procedures that utilize revascularization techniques, such as bypass grafting, are performed annually to treat cardiovascular disease.[1] Current clinical conduits for small-diameter (<6 mm) bypass grafting such as the saphenous vein are limited in their availability and can become compromised due to narrowing induced by intimal hyperplasia.[2,3] In addition, synthetic grafts—another common clinical vascular conduit—can fail due to thrombosis in small-diameter applications despite their success in large-diameter situations.[4,5] Autologous cell-based tissue engineering, which aims to develop functional native-like tissue mimics, is a promising alternative having shown both reduced intimal hyperplasia and thrombosis.[6–9] However, despite the advances seen in this field, many designs fail to assess cells from realistic clinical populations.

Many preclinical evaluations of cell-based small-diameter tissue-engineered vascular grafts (TEVGs) utilize cells from healthy humans or animals.[6–12] While these studies have shown that seeding scaffolds with autologous cells promote patency and regenerative effects seen in TEVGs, these

[1]Department of Bioengineering, University of Pittsburgh, Pittsburgh, Pennsylvania.
[2]McGowan Institute for Regenerative Medicine, University of Pittsburgh, Pittsburgh, Pennsylvania.
[3]Department of Plastic Surgery, University of Pittsburgh, Pittsburgh, Pennsylvania.
[4]Division of Trauma Plastic Surgery, Department of Plastic and Reconstructive Surgery, Craniofacial Research Center, Chang Gung Memorial Hospital, Chang Gung University, Taoyuan, Taiwan.
[5]Department of Surgery, University of Pittsburgh, Pittsburgh, Pennsylvania.
[6]RiMED Foundation and DICGIM, University of Palermo, Italy.
[7]Center for Vascular Remodeling and Regeneration, University of Pittsburgh, Pittsburgh, Pennsylvania.
[8]Department of Cardiothoracic Surgery, University of Pittsburgh, Pittsburgh, Pennsylvania.
*These authors contributed equally to this work.

are not directly representative of a realistic clinical population such as those at high risk of cardiovascular disease. Diabetic[13] and elderly[14] individuals are two demographics that are at high risk for cardiovascular disease, and cells derived from these patient groups have specific deficits that bring their therapeutic utility into question. These include reduced proliferation, differentiation potential, ability to stimulate angiogenesis, and potency of secreted factors.[13,15–19] As the success of autologous engineering hinges on processes driven by a patient's own cells,[7,20–22] it is critical to evaluate the success of TEVGs constructed with human cells from clinically relevant donor populations to understand their suitability for autologous tissue engineering.

Stem cells such as the muscle-derived cells[9] and pericytes[10] previously utilized by our laboratory have been shown to possess regenerative properties capable of generating robust TEVGs and can be harvested without sacrifice of already existing vascular structures. However, adipose-derived mesenchymal stem cells (AD-MSCs) represent a more clinically ideal cell type for TEVGs, as these are more easily and plentifully harvested. In this study, we sourced human AD-MSCs from diabetic, elderly, and healthy patients to compare their *in vivo* effectiveness as a TEVG in our established rat model.[9,10] Before implantation, AD-MSCs from each donor cohort were analyzed for their ability to properly seed within scaffolds, and postimplantation TEVGs were analyzed for their patency and composition. The composition of each TEVG was assessed for the main vascular cell types (smooth muscle cells [SMCs], endothelial cells) and extracellular matrix components (collagen, elastin). In addition, as this study revealed that diabetic TEVGs are prone to failure from thrombotic occlusion, one potential mechanism, downregulated fibrinolysis, was investigated.

Materials and Methods

Isolation and culture of AD-MSCs

AD-MSCs were isolated from human patients using previously described methods.[19] Briefly, adipose tissue was obtained, minced, and then digested in a collagenase solution (1 mg/mL, type II) for 30 min. The solution was then filtered through gauze, centrifuged, resuspended in an NH4Cl erythrocyte lysis buffer (154 mM), and centrifuged again to obtain a cell pellet. That cell pellet was plated and cultured to obtain AD-MSCs. In this study, cells were used between passage numbers 4–6. AD-MSCs were cultured as previously described.[19]

AD-MSCs were isolated in accordance with an approved institutional review board exemption status protocol, only obtaining the following information to protect patient confidentiality: gender, age in years, presence of diabetic condition, and body mass index (BMI). For the purposes of this study, we classified donors into the following groups based on SCORE (Systematic Coronary Risk Evaluation[14]) charts provided by the European Society of Cardiology for risk of cardiovascular disease: ''healthy'' (<45 years of age, nondiabetic), ''diabetic'' (<45 years of age, diabetic), and ''elderly'' (>60 years of age, nondiabetic). Diabetic and elderly groups were considered as high cardiovascular risk, clinically relevant cohorts. The ages were kept similar in a younger bracket to isolate the effect of diabetes when comparing between healthy and diabetic, and likewise, when comparing between healthy and elderly, only nondiabetics were considered in each group. In addition, all cells were isolated from female patients to isolate gender effects (the topic of a separate study). BMI range was consistent between groups: 29.4 ± 4.8 (healthy), 26.7 ± 4.2 (diabetic), and 28.7 ± 0.8 (elderly). For a complete listing of donors, see Table 1.

Scaffold fabrication

Bilayered, tubular, biodegradable, elastomeric scaffolds (1.3 mm ID, 10 mm length) were created from poly(ester urethane)urea (PEUU) as previously described.[23,24] PEUU was synthesized based on polycaprolactone diol, 1,4-diisocyanatobutane, and putrescine and then fabricated in two distinct layers, a design that has been used by our team in prior studies.[9,10,24] The inner layer was fabricated using thermally induced phase separation (TIPS) that creates a porous layer to facilitate cell seeding and integration, which was then finished with an electrospun (ES) outer layer to provide mechanical stability ($\sim$400 μm TIPS thickness, $\sim$70 μm ES thickness[10]).

Cell seeding

AD-MSCs were seeded into PEUU scaffolds using our rotational vacuum seeding device, which has been previously

Table 1. AD-MSC Human Donor Information

Gender	*Age*	*Diabetic*	*BMI*
	Healthy donors		
F	38	No	33.0
F	35	No	28.6
F	33	No	29.9
F	32	No	21.4
F	26	No	32.6
F	40	No	25.5
F	38	No	35.2
Average	34 ± 5		29.4 ± 4.8
	Diabetic donors		
F	43	Yes	22.2
F	45	Yes	30.6
F	39	Yes	27.4
F	39	Yes	23.7
Average	42 ± 3		26.0 ± 3.8
	Elderly donors		
F	68	No	28.8
F	65	No	27.8
F	64	No	29.8
F	61	No	28.3
Average	65 ± 3		28.7 ± 0.8

Human AD-MSCs were isolated from healthy ($n=7$), diabetic ($n=4$), or elderly ($n=4$) patients. Body mass index (BMI) was similar between groups, and confounding factors were removed when comparing between groups (i.e., age was kept similar in the defined younger classification (<45 years) when comparing between healthy and diabetic, while nondiabetic status was kept constant when comparing healthy and elderly).

AD-MSC, adipose-derived mesenchymal stem cells.

described and validated.[25] Briefly, scaffolds were mounted within the chamber of the device and infused lumenally at a rate of 2 mL per minute with a cell suspension containing 3 million AD-MSCs (suspension concentration: 1 million cells/mL, total volume: 3 mL). During cell infusion, the chamber was closed, and a vacuum force of −127 mmHg was applied. Following seeding, constructs were placed within static media for 4 h to allow for cellular adhesion before being placed within 500-mL spinner flasks (Kontes #Cytostir 882911-0250) for 48 h and stirred at 15 rpm, at which point the constructs were considered prepared for *in vivo* implantation.

As a means to ensure that cell seeding was not altered across AD-MSC donor groups causing confounding effects during *in vivo* studies, seeded constructs from each group (healthy, diabetic, elderly) were created. To analyze cell seeding, sections were stained with DAPI to identify cell nuclei and F-actin (Phalloidin, 1:250; Sigma #P5282) to show cellular spreading along scaffolding material. Images were acquired at 10× using an epifluorescent microscope with NIS Elements software (version 4, Nikon Instruments, Inc.). Images were then analyzed using toolboxes and custom scripts in ImageJ (1.47; Rasband) to analyze cell density. Briefly, images were stitched together to acquire complete cross-sectional views upon which they were virtually segmented into circumferential or radial pieces. Cell densities per area were measured comparing all directions (i.e., radial, circumferential, and longitudinal).

In vivo *implantation and explant*

Seeded scaffolds constructed from cells from all patients in Table 1 were implanted as abdominal aortic interposition grafts in Lewis rats for 8 weeks as previously described.[9,10] Briefly, rats were placed under anesthesia (4% isoflurane and 50 mg/kg ketamine for induction; 1% isoflurane for maintenance) and administered cefazolin (100 mg/kg, intramuscular) as a prophylactic. Microsurgical techniques were performed to suture a seeded construct as an end-to-end anastomosis with interrupted 10-0 Prolene sutures. After the graft was secured, the patency of the graft was verified by direct observation of distal pulse pressure. Antiplatelet therapy was provided for 1 month postsurgery (dipyridamole 250 mg/kg for 7 days, 100 mg/kg for the following 3 weeks; aspirin 200 mg/kg for 7 days, 100 mg/kg for the following 3 weeks). All implantations were carried out to an 8-week time point, unless obvious distress of the rats was noticed due to thrombotic complications, at which point animals were euthanized. Upon euthanasia, angiography was performed to assess patency of the TEVG upon which it was explanted. All explanted TEVGs were fixed in 4% paraformaldehyde for 30 min, bathed in 30% sucrose for 30 min, and then frozen for histologic analysis. Native aortas were explanted from nonoperated rats for comparisons as a positive control.

It is important to note that one of the TEVGs in our study from the elderly group was patent but aneurysmally dilated upon explant; on histological examination, the ES layer was abnormally fragmented. This was an anomaly that has not been observed in any of our previous studies,[9,10] and so, this sample was excluded from analysis of composition.

Histologic evaluation, immunofluorescence, and multiphoton microscopy

Frozen TEVGs were sectioned through cryomicrotome and mounted on gelatin-coated slides. Sections were then stained with hematoxylin and eosin or immunofluorescent chemistry using standard techniques. Antibodies were used to detect the presence of endothelial cells (ECs) (von Willebrand Factor [vWF]–1:250; US Biological #V2700-07), SMCs (smooth muscle alpha-actin [SMA]–1:1000; Sigma #A5228 and calponin–1:250; Abcam #ab46794), and elastin (1:100; EPC #RA75) with fluorescent secondary antibodies (Rockland #611-1202 [1:1000]; Invitrogen #A10521 [1:1000], Sigma #C2821 [1:300]). All images were acquired at 20× using an epifluorescent microscope with NIS Elements software. Analysis was restricted to the newly developed luminal tissue within TEVGs (Fig. 2D).

To analyze the presence of collagen, we utilized multiphoton microscopy as previously described.[26] Briefly, an Olympus multiphoton microscope (Model FV10, ASW software; Olympus America, Inc.) was used to image collagen fibers using second-harmonic generation (excitation wavelength: 780 nm, emission wavelength: 400 nm) acquired at 25× magnification.

Fibrinogen zymography

To examine the mechanisms of thrombotic failure observed when utilizing diabetic AD-MSCs and as a means to analyze the fibrinolytic potential of MSC secreted factors, zymography was performed utilizing fibrinogen-doped acrylamide gels using previously established techniques.[27] Briefly, fibrinogen (final concentration: 5.33 μg/mL; Sigma #F8630) was incorporated into the resolving portion of a 7.5% polyacrylamide gel during polymerization. AD-MSC-conditioned media (mixed with 4× nonreducing Laemmli sample buffer [BioRad #161-0747]) were incubated at room temperature for 15 min followed by separation by SDS-PAGE. Gels then underwent several washes in water and 2.5% Triton-X before incubation in a divalent cation reaction buffer (50 mM Tris-HCl pH 7.4, 1 mM $CaCl_2$, 1 mM $MgCl_2$, 37°C). Digestions were performed for 7 days to allow for enzymatic degradation of the entrapped fibrinogen within the gel. Degradation occurs by active enzymes directly digesting fibrinogen or reacting indirectly with contaminating plasminogen present in the fibrinogen mixture. Gels were then stained with Blue BANDit Protein Stain (Amresco) to visualize degradation bands. The amount of degradation was quantified using gel analysis tools within ImageJ (National Institutes of Health) by integrating the mean grayscale intensity over the area of each band.

Fabrication of fibrin-based constructs

As a second means to investigate the fibrinolytic potential of AD-MSCs, the degradation of fibrin-based constructs entrapped with SMCs while being stimulated with AD-MSC-conditioned media was monitored. Fabrication of fibrin-based constructs containing entrapped SMCs was performed as previously described.[27] Briefly, fibrin gel constructs were created by immediately pipetting 200 μL of a polymerization mixture (3.7 mg/mL fibrinogen [Sigma

#F4753-5G], 0.2 U/mL thrombin [Sigma #T7513-500UN], 1.25 mM $CaCl_2$, and 50,000 cells/mL) into a circle etched on tissue culture plastic. Gels were then incubated (37°C for 30 min) to allow for polymerization before adding conditioned media. Nonconditioned media were used as control. In addition, to provide for a gradation in fibrinolysis, conditioned media were supplemented with the fibrinolytic inhibitor, ε-amino caproic acid (ACA, 0.5, 1.0, or 3.0 mM). All samples were repeated in triplicate using $n=3$ donors per group.

To analyze the degradation of each gel, images were taken with a 16 megapixel camera at 1, 4, and 7 days. To quantify this degradation, which appeared as the gels developing a porous structure and becoming increasingly translucent, mean grayscale intensity measurements of each gel image were made in ImageJ. Gels that had a lower intensity were more translucent and considered as more degraded. Samples incubated without ACA were found to catastrophically detach from the edges rather than showing a smooth change in translucence.

Quantification of urokinase plasminogen activator activity in conditioned media

A fluorometric microplate kit was utilized to detect the level of urokinase plasminogen activator (uPA) activity within conditioned media samples (AnaSpec, #72159). All protocols were followed according to the manufacturer's instructions. All samples were repeated in triplicate using $n=4$ donors per group.

Statistics

All statistical analyses were performed utilizing Minitab (version 16; Minitab, Inc.) to perform either a one-way ANOVA or a Student's *t*-test. A statistically significant difference was defined as $p<0.05$. All data are expressed as mean ± standard deviation. All data were checked for the assumptions of normality and homogeneity of variance.

Results

(1) AD-MSCs from healthy, diabetic, and elderly donors all seed scaffolds similarly

As a point of quality control and to verify that cell seeding was consistent, we analyzed AD-MSC-seeded scaffolds from each patient cohort (healthy, diabetic, or elderly; $n=3$ per group). In all cases, AD-MSCs were able to successfully seed scaffolds at high efficiency (>95% of the infused cells became entrapped within scaffolds) and uniformity (Fig. 1A–C). Of note, the cells were appreciably spread on the scaffold after dynamic culture. Quantitatively comparing the cell density per area in the longitudinal, circumferential, and radial directions confirmed this uniformity. As an example, when cross-section images were segmented into three radial pieces, approximately one-third (~33%) of the total cells fell into each segment (Fig. 1D). In all cases, a nonsignificant *p*-value was shown through one-way ANOVA (radial: 0.94, 0.75, 0.77; circumferential: 0.96, 0.48, 0.65; longitudinal: 0.76, 0.05, 0.26; for healthy, diabetic, and elderly, respectively) indicating uniformity.

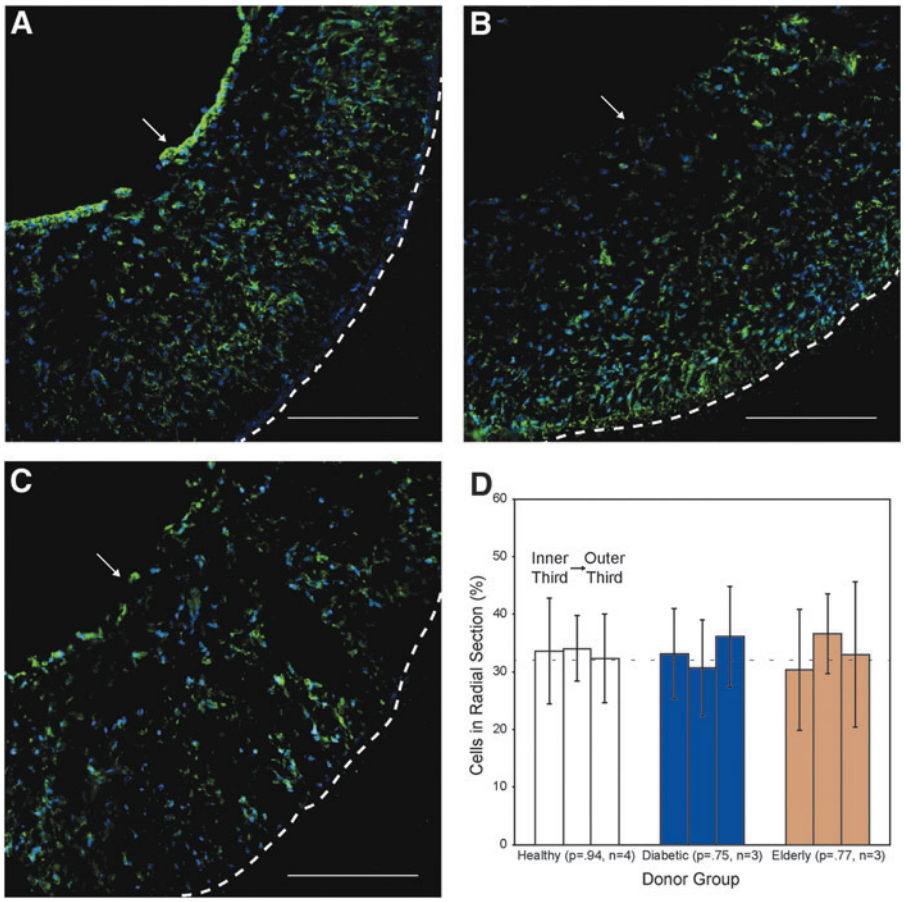

FIG. 1. AD-MSCs from healthy, diabetic, and elderly donors successfully seed within scaffolds. AD-MSCs from healthy **(A)**, diabetic **(B)**, and elderly **(C)** donors were seeded into scaffolds ($n=3$) and stained for cell nuclei (*blue*: DAPI) and F-actin (*green*: Phalloidin). All scaffolds showed a uniform distribution of cells and consistent spreading along the scaffold. *White arrow* indicates the lumen and the *dashed line* indicates outer border of the scaffold. Scale bar = 200 μm. **(D)** A uniform radial distribution of cells seeded into the scaffold was determined by measuring cell numbers (presented as mean percentage of total ± SD) in sections defined by each third thickness in comparison to a perfectly even distribution (*dashed line*). No significant difference was observed ($p>0.05$). AD-MSCs, adipose-derived mesenchymal stem cells; SD, standard deviation. Color images available online at www.liebertpub.com/tea

(2) TEVGs seeded with AD-MSCs from nondiabetic donors displayed a high patency rate at an 8-week time point, whereas a low patency rate was observed when AD-MSC from diabetic donors were utilized; thrombotic occlusion was responsible for decreased patency

Obvious blood flow was noted by a strong distal pulse pressure in all grafts upon implantation. At the 8-week endpoint of the study, patency was assessed using angiography, and only patent TEVGs exhibited flow of the contrast agent past the graft to the hind legs (Fig. 2A). Investigating the effect of donor group revealed that whereas healthy and elderly AD-MSCs were able to produce patent vessels 100% and 71% of the time, respectively, diabetic AD-MSCs had a markedly reduced patency rate of 28% (Fig. 2B). Nearly all animals with nonpatent grafts showed occlusion-related symptoms at acute time points (<1 week) at which point they were explanted. A single animal, with AD-MSCs from diabetic donors, remained free of symptoms for 8 weeks despite full occlusion of the graft. Gross observation of all occluded grafts revealed the presence of a lumenal clot (Fig. 2C). Patent grafts displayed significant remodeling with a tissue-like appearance in the generation of TEVGs, whereas nonpatent grafts—even the one that was explanted after 8 weeks—exhibited no such tissue-like appearance (Fig. 2D). In particular, a newly developed vascular-like neotissue developed lumenally, and the PEUU scaffold TIPS layer showed visual signs of degradation.

(3) All patent TEVGs acquire the presence of vascular cellular and extracellular components regardless of donor group

To determine which types of cells incorporated into the TEVG, and the extent of incorporation, we performed immunofluorescent chemistry for the presence of vascular SMCs (SMA, calponin) and endothelial cells (vWF). In all patent explanted TEVGs, a composition with the majority of the tissue thickness comprising SMCs (SMA and calponin positive) and a continuous lining of vWF-positive endothelial

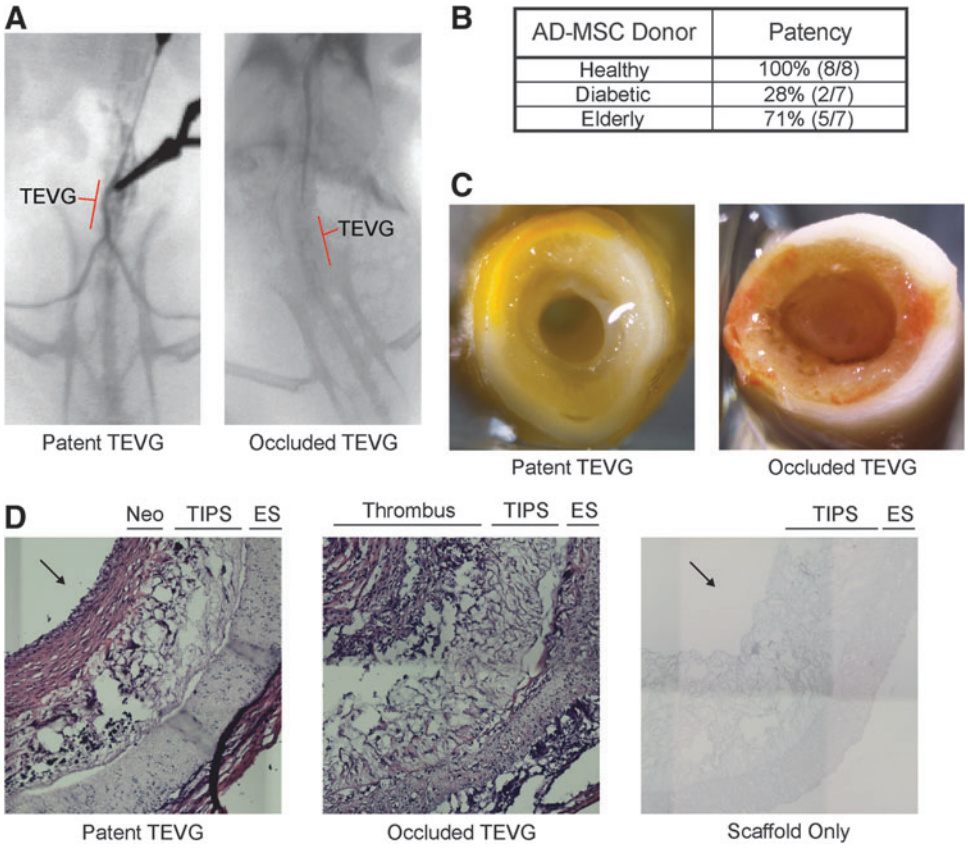

FIG. 2. Diabetic AD-MSCs do not produce patent vessels, whereas healthy and elderly do. **(A)** Angiograms were performed to assess the patency of TEVGs at the 8-week endpoint with a patent vessel showing clear flow past the graft to the hindquarters. **(B)** Total patency rate was calculated based on the number of patent versus total TEVGs; note that TEVGs created using cells from diabetic donors show a marked reduction in patency. **(C)** Gross inspection of the explants revealed that the primary reason for nonpatent TEVGs was occlusive thrombosis. **(D)** Hematoxylin and eosin-stained sections of a patent 8-week TEVG, a nonpatent 8-week TEVG, and a nonimplanted PEUU scaffold. Significant remodeling of patent TEVGs included newly developed neotissue (Neo) lumenally and breakdown of the original PEUU scaffolding material (inner layer: TIPS, outer layer: ES). Occluded grafts displayed the presence of a thrombus and no remodeling. *Arrows* indicate lumen in Figure 2D. ES, electrospun; PEUU, poly(ester urethane)urea; TEVGs, tissue-engineered vascular grafts; TIPS, thermally induced phase separation. Color images available online at www.liebertpub.com/tea

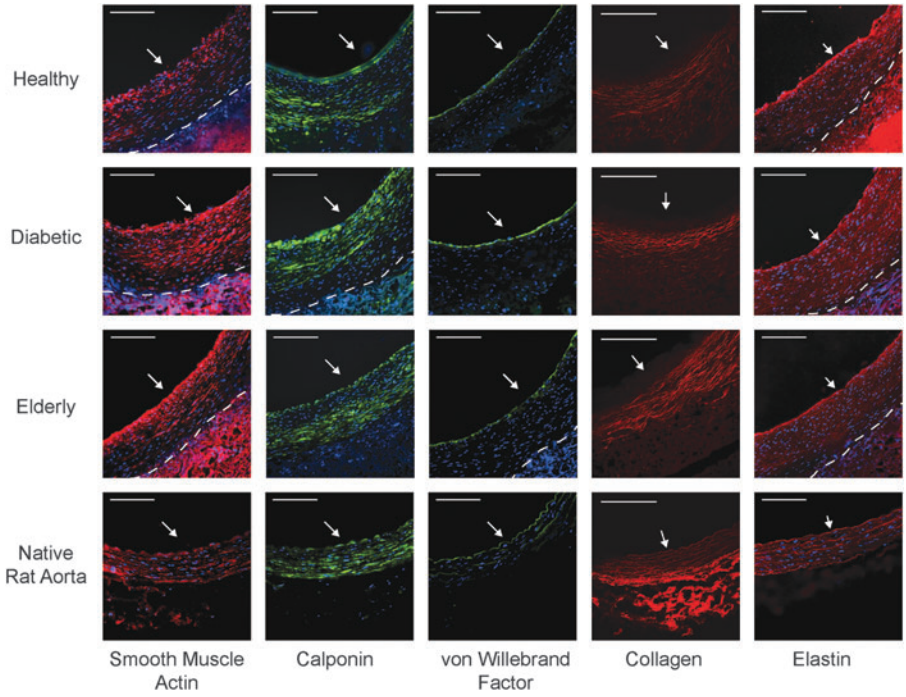

FIG. 3. All patent TEVGs have a composition consisting of vascular cells and extracellular matrix. Patent TEVGs, regardless of AD-MSC donor type, display significant remodeling with the development of neotissue composed of smooth muscle alpha-actin-positive (*red*; *first column*) and calponin-positive (*green*; *second column*) smooth muscle cells, as well as a continuous lining of von Willebrand Factor-positive ECs (*green*; *third column*), which are present in native arteries (*bottom row*). In addition, TEVGs, regardless of AD-MSC donor type, display a development of a fibrous, circumferentially aligned collagen network (*red*; *fourth column*). Finally, TEVGs, regardless of AD-MSC donor type, display alpha-elastin throughout the neotissue thickness (*red*; *fifth column*), including a prominent layer next to the lumen. However, the prominent medial elastic lamellae, which are present in native arteries, were absent in remodeled TEVGs. All immunofluorescent images were counterstained for cell nuclei (*blue*: DAPI). *White arrow* indicates the lumen, and the *dashed line* indicates the boundary between neotissue and residual TIPS. Scale bar = 100 μm. Note that the residual PEUU scaffolding material produces a significant amount of autofluorescence and should not be regarded as positive staining in these images. Color images available online at www.liebertpub.com/tea

cells along the lumen was observed (Fig. 3; native artery included for comparison).

To determine the extent of scaffold remodeling—that is, replacement of PEUU polymer with new extracellular matrix—we performed two forms of microscopic analysis. Multiphoton microscopy was utilized to image collagen, which displayed a fiber-like structure (Fig. 3). Of note is that collagen fibers were not present entirely throughout the thickness as they were in native arteries; specifically, they were absent near the lumen (data not shown). In addition, immunofluorescent chemistry was used to detect the presence of elastin within explanted vessels, which was observed throughout the thickness of TEVG neotissue, similar to native artery controls (Fig. 3). However, despite the immunological presence of elastin in TEVGs, the pronounced elastic lamellae of native arteries were not observed.

(4) AD-MSCs from diabetic donors produced less fibrinolytic factors than AD-MSCs from healthy donors

To test a potential mechanism for the prominent thrombosis observed when using diabetic AD-MSCs, activation of the fibrinolytic pathway by AD-MSCs was monitored *in vitro*. This pathway operates *in vivo* as a proteolytic cascade ultimately leading to activation of plasmin and digestion of the fibrin-rich thrombus. Activity of this cascade is regulated by multiple species, including two plasminogen activators (uPA and tissue plasminogen activator) and various inhibitors (e.g., plasminogen activator inhibitor, soluble uPA receptor, α_2-antiplasmin). To screen for fibrinolytic factors potentially secreted by AD-MSCs, which may be diminished in the diabetic case, fibrinogen zymography was used. Following 7 days of enzymatic reaction, clear degradation bands were seen at molecular weights of 31, 40, 85, 150, and 250 kD (Fig. 4A). Visual comparisons show that media conditioned by AD-MSCs from healthy donors produced prominent bands at 31 kD and 40 kD, whereas media conditioned by AD-MSCs from diabetic donors did not. Quantifying the band areas at these molecular weights revealed a significant difference between the healthy and diabetic groups with an additional difference in the band at 150 kD (Fig. 4B). Development of the zymograms for shorter periods (1 or 3 days) revealed less prominent degradation bands (data not shown).

As a means to show that healthy AD-MSCs produced more potent fibrinolytic factors than those isolated from diabetic patients, we created fibrin-based constructs containing SMCs and exposed them to AD-MSC-conditioned media. SMCs can be inherently fibrinolytic, and so, this assay was meant to address how AD-MSCs in a vascular

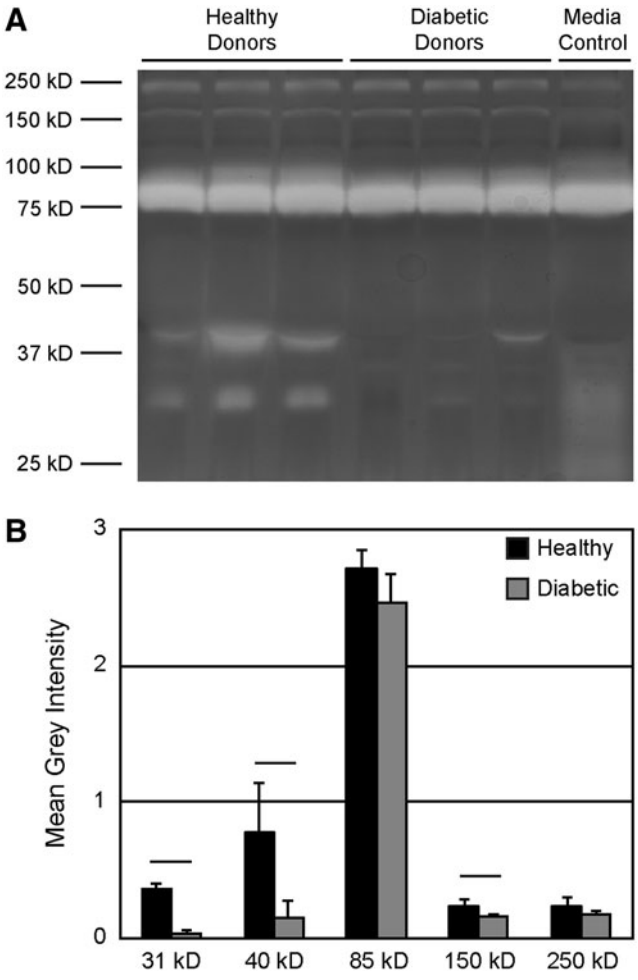

FIG. 4. Diabetic AD-MSCs produce less fibrinolytic factors than healthy AD-MSCs. **(A)** Zymography was performed utilizing conditioned media from AD-MSCs from healthy or diabetic donors using acrylamide gels doped with fibrinogen. *White bands* indicate areas of fibrinogen degradation, several of which were more prominent when AD-MSCs from healthy donors were used. Media control = nonconditioned serum-containing media. **(B)** *Bands* were quantified using toolboxes within ImageJ; bands at 31, 40, and 150 kD were increased in healthy samples. Data are presented as mean ± SD. *Black bar* = statistically significant difference ($p < 0.05$).

graft might mediate the fibrinolytic potential of host SMCs. In the absence of ACA, catastrophic detachment and compaction of constructs due to a high degree of degradation were observed upon stimulation with media conditioned by healthy AD-MSCs (Fig. 5A). This effect was reduced by using media conditioned by cells from diabetic patients (Fig. 5A). It is important to note that AD-MSC-based gels did not detach or substantially degrade (data not shown).

As the degradation of these gels occurred so rapidly, we treated a separate set of constructs with varying concentrations of the fibrinolytic inhibitor ACA. This was intended to allow visual resolution of the degradation rate differences between the healthy and diabetic groups. Inhibiting degradation with 3 mM ACA was sufficient to prevent any degradation over 7 days regardless of group (Images in Fig. 5B, quantification in Fig. 5C). On the contrary, inhibiting with 0.5 mM ACA was not sufficient to differentiate between the healthy and diabetic groups. The intermediate inhibitor concentration of 1 mM revealed a significant difference between the fibrinolytic behavior of the healthy and diabetic groups, particularly at the 4- and 7-day time points (Fig. 4B, day 1 and 4 data are presented in Supplementary Fig. S1; Supplementary Data are available online at www.liebertpub.com/tea). This indicates that AD-MSCs from healthy donors have a fibrinolytic activity strong enough to overcome inhibition by 1 mM of ACA, while cells from diabetic donors do not.

(5) uPA activity differed between AD-MSCs from healthy and diabetic donors

Prior literature[28,29] suggested that the identity of the 31 kD zymographic band (recall Fig. 4A) could be uPA. We were unable to detect uPA in conditioned media by Western blot (data not shown); however, we believe the levels of protein present in the media may have been below the detection limit for Western blot. To specifically detect uPA with high sensitivity, we used a fluorometric uPA activity assay kit. Conditioned media from both cell types displayed uPA-specific protease activity, but the activity of cells from diabetic patients was ~67% of that seen with cells from healthy patients (Fig. 6).

Discussion

In the current study, we have shown that scaffolds seeded with AD-MSCs from human patients can remodel into native-like TEVGs following 8 weeks of implantation. Among the three different donor populations analyzed—which included two cohorts at high cardiovascular risk—a low patency rate for the TEVGs was found only when using AD-MSCs from the diabetic cohort. TEVG failures were consistently due to thrombotic occlusion at an early time point. Throughout the study, we took measures to minimize confounding effects (e.g., using the same gender, avoiding overlapping age brackets between elderly and diabetic patients) and ensured that *in vivo* effects were not related to fabrication (i.e., poor or nonuniform cell seeding) of the vascular grafts. For the AD-MSC-based grafts that remained patent, remodeling resulted in a cellular composition and matrix structure closely mimicking those seen in native arteries. We note that there were some exceptions, such as the lack of a full-thickness distribution of collagen and pronounced elastic lamellae in the TEVG. However, we expect that the remodeling process is incomplete at 8 weeks, and further maturation will occur as several groups have shown that TEVG remodeling is a long-term process.[12,30,31] Finally, broad reduction of fibrinolysis in the diabetic AD-MSCs—and specifically decreased uPA activity—was shown offering one potential mechanistic explanation for thrombotic failure of diabetic TEVGs.

Since it is a common practice to use cells from healthy patients in preclinical studies,[6–12] we would contend that testing cells from the intended patient cohort (and therefore the source of autologous cells) is critical. In addition, while only AD-MSCs were tested in this study, other cell types routinely utilized in vascular engineering such as endothelial cells,[32–34] endothelial precursor cells,[35,36] and SMCs[33,34,37] can also be affected by donor demographics. Assessing what other high-risk donor populations could possess ineffective

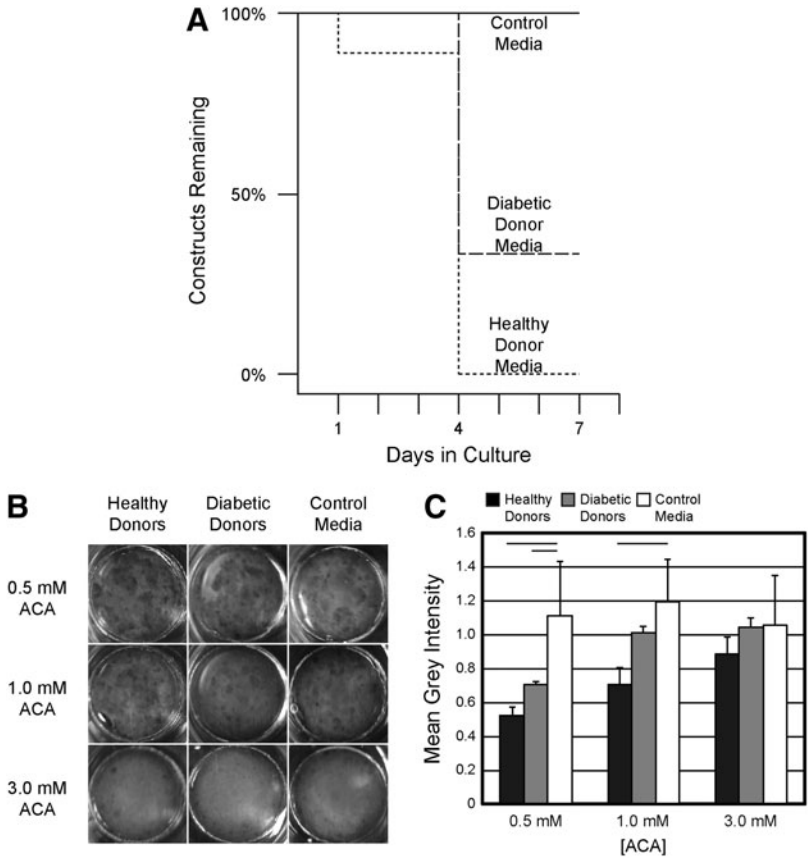

FIG. 5. Media conditioned by AD-MSCs from healthy donors promote higher degradation of fibrin-based constructs than media conditioned by AD-MSCs from diabetic donors. **(A)** Fibrin-based constructs were fabricated and cultured with control (non-conditioned) media or media conditioned by AD-MSCs from one of three healthy or diabetic donors. Each group was run in triplicate. The percentage of each set of nine constructs remaining at 1, 4, or 7 days is plotted by analogy to a ''survival curve'' to illustrate the loss of constructs when conditioned media were used. **(B)** To achieve a higher resolution on the degradation of fibrin constructs stimulated with AD-MSC-conditioned media, we inhibited gels with 0.5, 1, or 3 mM ε-amino caproic acid (ACA). Images are shown from an overhead view of fibrin disks at a 7-day time point. **(C)** Quantifying the mean grayscale intensity of each gel normalized to the background reveals that AD-MSCs from healthy patients promoted more fibrinolysis, when inhibited at an intermediate 1 mM ACA concentration. Images and measurements were also taken at days 1 and 4 and are shown in Supplementary Figure S1. Data are presented as mean ± SD. *Black bar* = statistically significant difference ($p < 0.05$).

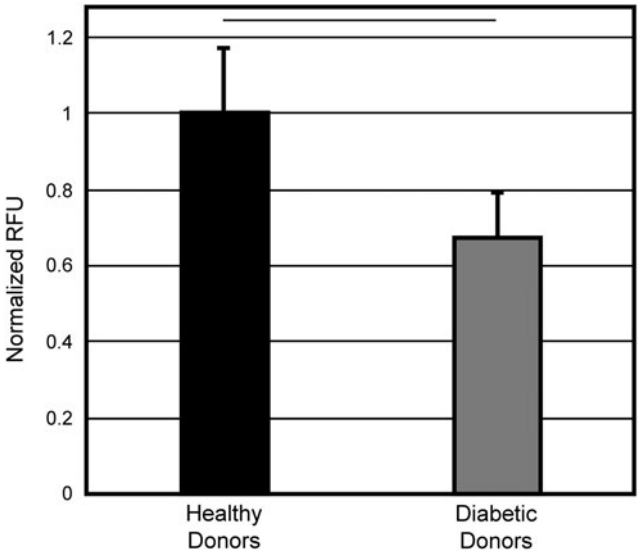

FIG. 6. Urokinase plasminogen activator (uPA) is responsible for the differences in fibrinolytic ability between AD-MSCs from healthy and diabetic donors. A uPA fluorometric microplate activity kit was performed on conditioned media samples. A significant reduction in uPA activity was observed when cells sourced from diabetic donors were used. Data are presented as mean ± SD. *Black bar* = statistically significant difference ($p < 0.05$).

cells for autologous grafts is a critical next frontier in autologous vascular engineering—and indeed for autologous regenerative medicine as a whole.

Cells from elderly patients induced successful remodeling of the scaffolds utilized for the TEVG. This was unexpected since in previous *in vitro* work,[19] AD-MSCs from elderly patients were defective at differentiating into SMCs and inducing SMC migration. Such effects on SMC composition are of primary importance to TEVG remodeling,[7,20–22] so we had expected less SMCs in the explanted grafts from the elderly cohort. There are a few possible explanations why the elderly derived cells worked in this *in vivo* model. One explanation relates to the concept of a ''critical size defect.'' In many models of tissue regeneration, the size of the defect may be small enough (and the host robust enough) that regeneration is successful, while beyond some size threshold, therapy is no longer effective. In the current study, we used a 1 cm long scaffold, which is significantly smaller than that required for a human-sized graft (on the order of 10 cm for a coronary artery bypass[3]). It may be that the *in vitro* deficiency we saw using AD-MSCs from elderly patients will become consequential upon moving to a larger sized graft and this should be explored. Another explanation could be the hemodynamic parameters of the rat interpositional implant model. While this model is useful for initial screening, the flow and coagulation pathways will be very different (and more similar to humans) in large animal models.[38,39] Therefore, large animal models will be needed to move this technology forward.

The results of this study also indicated the diminished fibrinolytic potential of diabetic AD-MSCs, which is further

corroborated by systemic reports of diabetic patients displaying a greater prothrombogenic phenotype with reduced fibrinolysis.[40,41] Studies have reported that diabetics have lower levels of fibrinolytic stimulators (tissue-type plasminogen activator[40]) and higher levels of fibrinolytic inhibitors (plasminogen activator inhibitor-1,[40,41] membrane uPA receptor,[42] and soluble uPA receptor[43]), which contribute to an overall reduction in fibrinolysis. In addition, studies have shown other fibrinolytic factors altered specifically in AD-MSCs from diabetic donors such as thrombospondin,[44] tissue-type plasminogen activator,[45] and plasminogen activator inhibitor-1.[45] However, to the best of our knowledge, our work is the first report to highlight a reduction in uPA activity by AD-MSCs from diabetic donors and the first to implicate a donor-linked stem cell deficiency as a method of TEVG failure. One limitation in these experiments is that we have not conclusively identified the 40 kD band, which differs in abundance between the two groups of cells. Literature reports suggest that this band could be the tissue-type plasminogen activator[46]; however, we were unable to confirm this through Western blot, potentially due to the low concentration of tissue-type plasminogen activator in conditioned media.

In conclusion, we performed an *in vivo* study investigating the ability of single-donor human AD-MSCs from two clinically relevant cohorts—diabetics and the elderly—to perform in the context of a TEVG. We demonstrated that while there was high graft patency when using AD-MSCs from nondiabetic patients, cells from diabetics were associated with a reduced success rate due to acute thrombosis, which could be mechanistically explained by reduced fibrinolytic activity. However, we have shown microscopic evidence that all patent grafts in our study were able to develop into robust TEVGs containing key vascular components such as SMCs, endothelial cells, collagen, and elastin allowing us to pursue modulations of the fibrinolytic pathway as a method to enable TEVG therapy for diabetic patients. Finally, the results of this study highlight the critical need to test cells from realistic patient populations when designing autologous therapies.

Acknowledgments

We thank Dr. Wendy Mars (University of Pittsburgh) for helpful discussions about plasminogen activation. This work was supported by the American Heart Association (AHA #12PRE12050163 to JTK) and National Institutes of Health (R21 #EB016138 to DAV, T32 HL094295 to JTK).

Disclosure Statement

No competing financial interests exist.

References

1. Lloyd-Jones D, Adams R, Carnethon M, De Simone G, Ferguson TB, Flegal K, Ford E, Furie K, Go A, Greenlund K, Haase N, Hailpern S, Ho M, Howard V, Kissela B, Kittner S, Lackland D, Lisabeth L, Marelli A, McDermott M, Meigs J, Mozaffarian D, Nichol G, O'Donnell C, Roger V, Rosamond W, Sacco R, Sorlie P, Stafford R, Steinberger J, Thom T, Wasserthiel-Smoller S, Wong N, Wylie-Rosett J, Hong Y; American Heart Association Statistics Committee and Stroke Statistics Subcommittee. Heart disease and stroke statistics-2009 update: a report from the american heart association statistics committee and stroke statistics subcommittee. Circulation **119,** E182, 2009.
2. Weintraub, W.S., Jones, E.L., Craver, J.M., and Guyton, R.A. Frequency of repeat coronary-bypass or coronary angioplasty after coronary-artery bypass-surgery using saphenous venous grafts. Am J Cardiol **73,** 103, 1994.
3. Waller, B.F., and Roberts, W.C. Remnant saphenous veins after aortocoronary bypass grafting: analysis of 3,394 centimeters of unused vein from 402 patients. Am J Cardiol **55,** 65, 1985.
4. Klinkert, P., Post, P.N., Breslau, P.J., and van Bocke, J.H. Saphenous vein versus ptfe for above-knee femoropopliteal bypass. A review of the literature. Eur J Vasc Endovasc Surg **27,** 357, 2004.
5. Desai, M., Seifalian, A.M., and Hamilton, G. Role of prosthetic conduits in coronary artery bypass grafting. Eur J Cardiothorac Surg **40,** 394, 2011.
6. Cho, S.W., Lim, S.H., Kim, I.K., Hong, Y.S., Kim, S.S., Yoo, K.J., Park, H.Y., Jang, Y., Chang, B.C., Choi, C.Y., Hwang, K.C., and Kim, B.S. Small-diameter blood vessels engineered with bone marrow-derived cells. Ann Surg **241,** 506, 2005.
7. Hibino, N., Yi, T., Duncan, D.R., Rathore, A., Dean, E., Naito, Y., Dardik, A., Kyriakides, T., Madri, J., Pober, J.S., Shinoka, T., and Breuer, C.K. A critical role for macrophages in neovessel formation and the development of stenosis in tissue-engineered vascular grafts. FASEB J **25,** 4253, 2011.
8. Krawiec, J.T., and Vorp, D.A. Adult stem cell-based tissue engineered blood vessels: a review. Biomaterials **33,** 3388, 2012.
9. Nieponice, A., Soletti, L., Guan, J.J., Hong, Y., Gharaibeh, B., Maul, T.M., Huard, J., Wagner, W.R., and Vorp, D.A. In vivo assessment of a tissue-engineered vascular graft combining a biodegradable elastomeric scaffold and muscle-derived stem cells in a rat model. Tissue Eng Part A **16,** 1215, 2010.
10. He, W., Nieponice, A., Soletti, L., Hong, Y., Gharaibeh, B., Crisan, M., Usas, A., Peault, B., Huard, J., Wagner, W.R., and Vorp, D.A. Pericyte-based human tissue engineered vascular grafts. Biomaterials **31,** 8235, 2010.
11. L'Heureux, N., Dusserre, N., Konig, G., Victor, B., Keire, P., Wight, T.N., Chronos, N.A., Kyles, A.E., Gregory, C.R., Hoyt, G., Robbins, R.C., and McAllister, T.N. Human tissue-engineered blood vessels for adult arterial revascularization. Nat Med **12,** 361, 2006.
12. Kelm, J.M., Emmert, M.Y., Zürcher, A., Schmidt, D., Begus Nahrmann, Y., Rudolph, K.L., Weber, B., Brokopp, C.E., Frauenfelder, T., and Leschka, S. Functionality, growth and accelerated aging of tissue engineered living autologous vascular grafts. Biomaterials **33,** 8277, 2012.
13. Dokken, B.B. The pathophysiology of cardiovascular disease and diabetes: beyond blood pressure and lipids. Diabetes Spectr **21,** 160, 2008.
14. Conroy, R., Pyörälä, K., Fitzgerald, AP, Sans, S., Menotti, A., De Backer, G., De Bacquer, D., Ducimetiere, P., Jousilahti, P., and Keil, U. Estimation of ten-year risk of fatal cardiovascular disease in europe: the score project. Eur Heart J **24,** 987, 2003.
15. Stolzing, A., Sellers, D., Llewelyn, O., and Scutt, A. Diabetes induced changes in rat mesenchymal stem cells. Cells Tissues Organs **191,** 453, 2010.

16. Cianfarani, F., Toietta, G., Di Rocco, G., Cesareo, E., Zambruno, G., and Odorisio, T. Diabetes impairs adipose tissue–derived stem cell function and efficiency in promoting wound healing. Wound Repair Regen **21,** 545, 2013.
17. Madonna, R., Renna, F.V., Cellini, C., Cotellese, R., Picardi, N., Francomano, F., Innocenti, P., and De Caterina, R. Age-dependent impairment of number and angiogenic potential of adipose tissue-derived progenitor cells. Eur J Clin Invest **41,** 126, 2011.
18. Schipper, B.M., Marra, K.G., Zhang, W., Donnenberg, A.D., and Rubin, J.P. Regional anatomic and age effects on cell function of human adipose-derived stem cells. Ann Plast Surg **60,** 538, 2008.
19. Krawiec, J.T., Weinbaum, J.S., St. Croix, C.M., Phillippi, J.A., Watkins, S.C., Rubin, J.P., and Vorp, D.A. A cautionary tale for autologous vascular tissue engineering: impact of human demographics on the ability of adipose-derived mesenchymal stem cells to recruit and differentiate into smooth muscle cells. Tissue Eng Part A **21,** 426, 2014.
20. Roh, J.D., Sawh-Martinez, R., Brennan, M.P., *et al.* Tissue-engineered vascular grafts transform into mature blood vessels via an inflammation-mediated process of vascular remodeling. Proc Natl Acad Sci U S A **107,** 4669, 2010.
21. Hashi, C.K., Zhu, Y.Q., Yang, G.Y., Young, W.L., Hsiao, B.S., Wang, K., Chu, B., and Li, S. Antithrombogenic property of bone marrow mesenchymal stem cells in nanofibrous vascular grafts. Proc Natl Acad Sci U S A **104,** 11915, 2007.
22. Hibino, N., Villalona, G., Pietris, N., *et al.* Tissue-engineered vascular grafts form neovessels that arise from regeneration of the adjacent blood vessel. FASEB J **25,** 2731, 2011.
23. Guan, J., Fujimoto, K.L., Sacks, M.S., and Wagner, W.R. Preparation and characterization of highly porous, biodegradable polyurethane scaffolds for soft tissue applications. Biomaterials **26,** 3961, 2005.
24. Soletti, L., Hong, Y., Guan, J., Stankus, J.J., El-Kurdi, M.S., Wagner, W.R., and Vorp, D.A. A bilayered elastomeric scaffold for tissue engineering of small diameter vascular grafts. Acta Biomater **6,** 110, 2010.
25. Soletti, L., Nieponice, A., Guan, J., Stankus, J.J., Wagner, W.R., and Vorp, D.A. A seeding device for tissue engineered tubular structures. Biomaterials **27,** 4863, 2006.
26. Tsamis, A., Phillippi, J.A., Koch, R.G., Pasta, S., D'Amore, A., Watkins, S.C., Wagner, W.R., Gleason, T.G., and Vorp, D.A. Fiber micro-architecture in the longitudinal-radial and circumferential-radial planes of ascending thoracic aortic aneurysm media. J Biomech **46,** 2787, 2013.
27. Ahmann, K.A., Weinbaum, J.S., Johnson, S.L., and Tranquillo, R.T. Fibrin degradation enhances vascular smooth muscle cell proliferation and matrix deposition in fibrin-based tissue constructs fabricated in vitro. Tissue Eng Part A **16,** 3261, 2010.
28. Andreasen, P.A., Kjoller, L., Christensen, L., and Duffy, M.J. The urokinase-type plasminogen activator system in cancer metastasis: a review. Int J Cancer **72,** 1, 1997.
29. Lijnen, H.R., Nelles, L., Holmes, W.E., and Collen, D. Biochemical and thrombolytic properties of a low molecular weight form (comprising leu144 through leu411) of recombinant single-chain urokinase-type plasminogen activator. J Biol Chem **263,** 5594, 1988.
30. Matsumura, G., Ishihara, Y., Miyagawa-Tomita, S., Ikada, Y., Matsuda, S., Kurosawa, H., and Shin'oka T. Evaluation of tissue-engineered vascular autografts. Tissue Eng **12,** 3075, 2006.
31. Wu, W., Allen, R.A., and Wang, Y. Fast-degrading elastomer enables rapid remodeling of a cell-free synthetic graft into a neoartery. Nat Med **18,** 1148, 2012.
32. Eringa, E.C., Serne, E.H., Meijer, R.I., Schalkwijk, C.G., Houben, A.J., Stehouwer, C.D., Smulders, Y.M., and van Hinsbergh, V.W. Endothelial dysfunction in (pre) diabetes: characteristics, causative mechanisms and pathogenic role in type 2 diabetes. Rev Endocr Metab Disord **14,** 39, 2013.
33. Kovacic, J.C., Moreno, P., Hachinski, V., Nabel, E.G., and Fuster, V. Cellular senescence, vascular disease, and aging part 1 of a 2-part review. Circulation **123,** 1650, 2011.
34. Kovacic, J.C., Moreno, P., Nabel, E.G., Hachinski, V., and Fuster, V. Cellular senescence, vascular disease, and aging part 2 of a 2-part review: clinical vascular disease in the elderly. Circulation **123,** 1900, 2011.
35. Tepper, O.M., Galiano, R.D., Capla, J.M., Kalka, C., Gagne, P.J., Jacobowitz, G.R., Levine, J.P., and Gurtner, G.C. Human endothelial progenitor exhibit impaired proliferation, cells from type ii diabetics adhesion, and incorporation into vascular structures. Circulation **106,** 2781, 2002.
36. Heiss, C., Keymel, S., Niesler, U., Ziemann, J., Kelm, M., and Kalka, C. Impaired progenitor cell activity in age-related endothelial dysfunction. J Am Coll Cardiol **45,** 1441, 2005.
37. Faries, P.L., Rohan, D.I., Takahara, H., Wyers, M.C., Contreras, M.A., Quist, W.C., King, G.L., and LoGerfo, F.W. Human vascular smooth muscle cells of diabetic origin exhibit increased proliferation, adhesion, and migration. J Vasc Surg **33,** 601, 2001.
38. Byrom, M.J., Bannon, P.G., White, G.H., and Ng, M.K. Animal models for the assessment of novel vascular conduits. J Vasc Surg **52,** 176, 2010.
39. Lewis, J., Van Thiel, D., Hasiba, U., Spero, J., and Gavaler, J. Comparative hematology and coagulation: studies on rodentia (rats). Comp Biochem Physiol Part A Physiol **82,** 211, 1985.
40. Carmassi, F., Morale, M., Puccetti, R., De Negri, F., Monzani, F., Navalesi, R., and Mariani, G. Coagulation and fibrinolytic system impairment in insulin dependent diabetes mellitus. Thromb Res **67,** 643, 1992.
41. Aso, Y., Matsumoto, S., Fujiwara, Y., Tayama, K., Inukai, T., and Takemura, Y. Impaired fibrinolytic compensation for hypercoagulability in obese patients with type 2 diabetes: association with increased plasminogen activator inhibitor-1. Metabolism **51,** 471, 2002.
42. Kenichi, M., Masanobu, M., Takehiko, K., Shoko, T., Akira, F., Katsushige, A., Takashi, H., Yoshiyuki, O., and Shigeru, K. Renal synthesis of urokinase type-plasminogen activator, its receptor, and plasminogen activator inhibitor-1 in diabetic nephropathy in rats: modulation by angiotensin-converting–enzyme inhibitor. J Lab Clin Med **144,** 69, 2004.
43. Eugen-Olsen, J., Andersen, O., Linneberg, A., Ladelund, S., Hansen, T., Langkilde, A., Petersen, J., Pielak, T., Møller, L., and Jeppesen, J. Circulating soluble urokinase plasminogen activator receptor predicts cancer, cardiovascular disease, diabetes and mortality in the general population. J Intern Med **268,** 296, 2010.
44. Varma, V., Yao-Borengasser, A., Bodles, A.M., Rasouli, N., Phanavanh, B., Nolen, G.T., Kern, E.M., Nagarajan, R.,

Spencer, H.J., 3rd, Lee, M.J., Fried, S.K., McGehee, R.E., Jr., Peterson, C.A., and Kern, P.A. Thrombospondin-1 is an adipokine associated with obesity, adipose inflammation, and insulin resistance. Diabetes **57,** 432, 2008.

45. Acosta, L., Hmadcha, A., Escacena, N., Perez-Camacho, I., de la Cuesta, A., Ruiz-Salmeron, R., Gauthier, B.R., and Soria, B. Adipose mesenchymal stromal cells isolated from type 2 diabetic patients display reduced fibrinolytic activity. Diabetes **62,** 4266, 2013.
46. Rijken, D.C., Hoylaerts, M., and Collen, D. Fibrinolytic properties of one-chain and two-chain human extrinsic (tissue-type) plasminogen activator. J Biol Chem **257,** 2920, 1982.

Address correspondence to:
David A. Vorp, PhD
Department of Bioengineering
University of Pittsburgh
Suite 300 Center for Bioengineering (CNBIO)
300 Technology Drive
Pittsburgh, PA 15219

E-mail: vorp@pitt.edu

Received: August 19, 2015
Accepted: April 12, 2016
Online Publication Date: May 5, 2016